MODAL DYNAMICS EXPERIMENT AND ANALYSIS OF A SUSPENSION ASSEMBLY USED IN HARD DISK DRIVES

Q. H. Zeng[1] and D. B. Bogy

Computer Mechanics Laboratory

Department of Mechanical Engineering

University of California

Berkeley, CA 94720

ABSTRACT

This report presents the investigation of the dynamic characteristics of a suspension assembly, called "Type 850AK", using both experimental and numerical techniques. Six samples with wires attached and no wires attached were measured to obtain statistical results. A parametric FE model of the assembly was developed. Good agreement between the FE model and the modal experiment was achieved. Using the model, the effects of the head load and the associated prestress and large deflection on the dynamics of the assembly were predicted. The load significantly affects the sway and second torsional modes. From the experiment and simulation it was found that the wire captures damaged the symmetry of the assembly. The sensitivity of the modal frequencies to the design variables was also investigated. Changes in the geometry of the bend region seriously affect the sway and torsional modes. The height of the ribs mainly affects the second and third bending modes, but it also affects the sway and torsional modes.

[1] Visiting scholar, Associate professor, Institute of Vibration Engineering, Nanjing University of Aeronuatics & Astronautics, Nanjing, China.

1. INTRODUCTION

Rigid disk drives contain high performance electromechanical components. One of the major components is the actuator mechanism that is used for high-accuracy and high-speed positioning of the sliders on the disks. Magnetic read/write heads are mounted onto the sliders. Miniaturized flexible arms, called suspensions, connect the sliders to the actuators. A suspension assembly consists of a base plate, a loadbeam, a flexure, and a slider. The suspension assembly is a critical component and serves some very important functions in the rigid disk drive (Miu, 1991). The suspension assembly must be compliant enough to follow undulations in the disk, and stiff enough to accurately and quickly position the slider. Therefore, a better understanding of the dynamics of the assembly is very important for disk drive design.

However, few research works in suspension dynamics, especially for the new type suspensions, are available. Early works are mainly related with the 3370-type and other older type suspensions. These works were reviewed in Miu's paper (1991). More recent contributions mainly focus on the following aspects. Jeans (1992) developed a finite element (FE) model of the Type 4 suspension, and calculated the sensitivity of modal frequencies to design parameters of the loadbeam. Yumura, et al. (1993) investigated the effects of the head load on the gain of the resonance, and proposed a new design method for in-line suspensions. The newly designed suspension had preferable properties because the torsional and lateral bending modes were decoupled. Wilson and Bogy (1994) studied the dynamic characteristics of the Type 3380 suspension assembly by modal experiment

and p-type finite element analysis. They (Wilson and Bogy, 1993) also analyzed the interaction of a 90mm disk and a Type 1650 suspension assembly by modal experiments. Harrison and Hanrahan (1995) investigated the effect of mandrel skew induced roll bias on suspension structural resonance.

The Type 850 suspension assembly was designed for mainstream desktop application, which is widely applied in the drives with 50% nano-sliders at present. The understanding of the dynamic properties of the assembly will be beneficial for the new drive design and redesign of the assembly. Therefore, we investigate the dynamics of the assembly in detail through both experimental and analytical methods. This report first describes the modal experiment of the assembly in its unloaded state. Six test samples were used to obtain the statistical results of the modal parameters for both cases of wires attached and without wires. Next, a parametric finite element model is created to analyze the assembly. The model was validated by the experimental results, and used to simulate the effects of wire captures, head load, and prestress with large deflection, on the dynamic properties. Finally, the sensitivity of the modal parameters to design variables of the assembly was studied.

2. Modal Experiment of the Type 850AK Suspension Assembly

2.1 Description and state of the assembly

The suspension assembly is shown in Figure 1. It is made up of a base plate, loadbeam, flexure and slider. The assembly is fixed to the actuator through the base plate. The

loadbeam is attached to the base plate by seven laser weld spots. The loadbeam contains a bend region and a rail. There is a formed section in the bend region to provide a vertical loading force (head load) when the assembly is installed in the drives. There are two ribs on the sides of the rail, which provide the stiffness to limit unwanted deflection. There are two wire captures on one of the ribs. The captures fix the wires to the rail. The flexure is welded to the loadbeam by two laser weld spots. A hemispherical pivot knob on the tab of the flexure, called a dimple, rests by simple contact on the bottom of the loadbeam. The slider, a 50% nano-slider, is glued to the flexure tab. The stiffness of the flexure controls the pitch and roll motion of the slider. During operation, the slider flies over the surface of the disk on the air bearing generated by the relative motion between the rotating disk and stationary slider.

The assembly in this study was mainly investigated in its unloaded state, that is, it was not deflected as if installed in the drive. The base plate was fixed. Using this configuration has three advantages. The first is the model created is required in the dynamic simulation of various disturbances (Hu and Bogy, 1995). The second is the boundary condition is easily implemented in the experiment and analysis, and can be accurately modeled. The third is that the other configurations, such as due to different head loads, and loading on the disk, can be conveniently analyzed through this configuration. One major disadvantage is that it is difficult to predict the damping properties of the other configurations from this configuration.

2.2 Experimental setup

Figure 2 shows a schematic representation of the experimental system utilized in the study. The system was totally described and verified in Zeng and Bogy (1996). The base excitation method was chosen to excite the assembly. The assembly was mounted onto a fixture, which was attached to a model 203 Ling Dynamics System Vibrator. An accelerometer mounted on the fixture was used to measure the base excitation motion in the Z direction. A Polytec Laser Doppler Vibrometer was used to measure the absolute velocity responses of the assembly. An HP3562A Dynamic Signal Analyzer was adopted for data acquisition and analysis to obtain the frequency response functions (FRFs) between the velocity responses and the acceleration of the base. Burst random signals were used in the excitation. The enhanced modal analysis software NAI-MODAL was applied in the geometric modeling of the assembly; controlling the analyzer; reading FRFs from the analyzer and storing FRFs and measurement parameters into a database; calibrating and modifying the FRFs; curve fitting; mode sorting; and mode shape animation.

2.3 Experimental procedure

In planning the experiment, we paid much attention to two aspects. The first was the manufacturing tolerances, which would result in the difference of the modal parameters from piece to piece. The experimental results of a specified piece would not represent the properties of the assembly. The second was the effects of the wires on the parameters, because it is difficult to accurately model their effects by the FE analysis. Therefore, six test samples were measured to obtain the statistical results. Using the same samples, those attached with wires were first measured, and then the samples were directly measured

again after the wires were removed. The effects of the wires can be understood by comparing the results.

The first sample was carefully measured. The geometric model, shown in Figure 3, consisted of 59 independent measurement points, and 19 dependent points. Points 5-40 are located on the loadbeam. Points 51-81 are located on the flexure. Points 82-89 are located on the slider. At points 86, 87, 88, 63, 64, 67, 32, 24, 9 and 11, the preliminary measurements were made in the frequency band of 0-16 kHz. Ten modes were found.

In the preliminary measurements we found that a suitable excitation level was essential for the experiment. This is because a higher level gives a higher signal/noise ratio. However, if the level was beyond a certain threshold value, the measured FRF showed a nonlinear phenomenon, even some modes would disappear. Figure 4 shows five FRFs measured at point 86 under five different excitation levels using the periodic chirp signals. The first curve was measured for the source level of the analyzer equal to 20 mV, and the velocity response was about 1.69 mm/s (peak). The first and second peaks of the curve correspond to the second bending and first torsional modes, respectively. The curve is not very smooth for the lower excitation level. The second curve, which was measured under the higher excitation level, is smooth. However, when the level was increased to 80 mV, the peaks of resonance in the measured FRFs became less distinct, and the curve shows a nonlinear property. When the level was equal to 140 mV, and the velocity response was about 9.6 mm/s, the two resonance peaks almost disappeared. This phenomenon results from the contacts between the flexure and the loadbeam at the

dimple. If the level exceeded the threshold value, the flexure and loadbeam would separate and impact each other at the dimple point, such that the assembly exhibits the non-linear property. The threshold value is dependent on many factors, such as the sample, mode, frequency band, and type of the excitation signal. The local modes relating to the slider are more sensitive to the excitation level. In the experiment, it is practical to decide the value through trial and error, based on the changes of the peaks of the measured FRFs after the source level of the analyzer is adjusted from a very small value to a larger value. In the unloaded state of the assembly, the threshold value was very small. Fortunately, in its loaded state, the threshold value is much larger. However, one should also pay attention to the phenomena in studying the dynamics of the assembly.

After the preliminary measurement, the frequency range 0-16 kHz was divided into five frequency bands: 180-380 Hz (mode 1 included), 700-2300 Hz (modes 2 and 3 included), 2200-3200 Hz (modes 4 and 5 included), 6000-10000 Hz (modes 6 and 7 included), and 9800-16050 Hz (three modes are included). For each band, the excitation levels (source levels) were carefully determined. Under control of the software, fifty-nine FRFs in each band were measured in the Z direction. The global orthogonal rational fractional polynorminal method was chosen to perform the curve fitting. The modal parameters were obtained by mode sorting. The measured mode shapes are shown in Figure 5.

Closely following the experiments of the assembly with wires attached as described above, we removed the wires, and performed the experiments again. The modal

parameters of the assembly with no wires attached were obtained. The mode shapes were very similar to the ones shown in Figure 5.

Considering the measured mode shapes, a simplified geometric model, which is shown in Figure 6, was created for the experiments of the remaining five samples. To reduce the work of the measurement, the number of independent measurement points was reduced to only 15. Using the above procedure, the modal parameters of the five samples with wires attached and with no wires attached were obtained.

2.4 Experimental results

Table 1 shows the mean values and standard deviations of the measured modal frequencies of the six samples. Table 2 shows the mean values and standard deviations of the measured damping ratios. The average mode shapes of the six samples were also obtained, which are similar to the ones shown in Figure 5. The slider's pitch mode was found only in two samples, so the deviations of the modal parameters of this mode are not presented in the tables. From Tables 1 and 2, and Figure 5, we can see that:

❶ There are no significant effects of the wires on the modal frequencies and mode shapes. The modal frequencies of the assembly with the wires attached are always smaller than the ones with no wires attached except for the first mode. That mainly results from the effects of the wire inertia. The largest difference is less than 2.8%.

❷ The modal damping ratios of the assembly with the wires attached are much larger than those with no wires attached. Except for the slider's roll and pitch modes, the average difference is about 200%.

❸ The measured mode shapes of the second bending and first torsional modes of all samples show the assemblies are not symmetric. The bending and torsional modes are coupled with each other. It should be mentioned that the assemblies without wires also exhibit similar properties. That means there are other factors that cause asymmetry of the assembly. This asymmetry could be harmful for the dynamics of the assembly because the torsional motion, which causes off-track errors (Yoneoka et al., 1989; Miu et al., 1990), will strongly be excited by vertical fluctuations when the torsional mode is coupled with the bending mode.

❹ The modal frequencies of the slider's roll and pitch modes vary significantly from sample to sample. This may indicate the differences of the static stiffness of roll and pitch, and the locations of the sliders.

❺ Mode 8 (10327Hz) appears to be a torsional mode from the measured mode shape, shown in Figure 5. However, it could be a torsional mode or a sway mode, or a coupled mode of torsion and sway.

3. Analysis of the Type 850AK Suspension Assembly

3.1 Parametric Model

The ANSYS Parametric Design Language (APDL) was applied to create an FE model of the Type 850AK suspension assembly, and analyze its dynamic properties. The APDL allows one to build the model in terms of variables, which in turn allows one to make design changes easily and conveniently, even to perform a design optimization. Using the APDL, a modeling procedure becomes a programming procedure. The obtained model is a program, so it is very convenient for us to investigate the dynamics of the assembly.

In modeling the assembly, it was first modeled assuming symmetry about the central line of the assembly. The global coordinate system XYZ was the same as the design coordinate system with its origin located at the center of the tooling hole. Four local coordinate systems were defined. About 75 variables were used to define the dimensions of the assembly, and create a solid model. As examples, the modeling procedures of the rib and bend region of the loadbeam are described as follows

Rib modeling. The first local coordinate system $X_1Y_1Z_1$ was defined at the global origin and rotating with the Y axis by an angle θ. In this system, the rail of the loadbeam was modeled. Figure 7 shows the modeling of the rib. Once given L_{T1},L_{T2}, β, R_H, α, R_R, and L_{RC} , based on the geometric relationship shown in Figure 7, the coordinates of the six key points can then be found as

$$\mathrm{P_{1I}}:(-L_{T1},\quad L_{T1}tg\beta+\frac{l_{RI}}{\cos\beta},\quad 0)$$

$$\mathrm{P_{1H}}:(-L_{T1},\quad L_{T1}tg\beta+\frac{l_{RH}}{\cos\beta},\quad R_H)$$

$P_{10}:(-L_{T1},\quad 0,\quad 0)$

$P_{2I}:(L_{T2},\quad -L_{T2}tg\beta+\frac{l_{RI}}{\cos\beta},\quad 0)$

$P_{2H}:(L_{T2},\quad -L_{T2}tg\beta+\frac{l_{RH}}{\cos\beta},\quad R_H)$

$P_{20}:(L_{T2},\quad 0,\quad 0)$

where

$$l_{RI}=L_{RC}+R_R tg\frac{\alpha}{2}$$

$$l_{RH}=L_{RC}+R_R tg\frac{\alpha}{2}+\frac{R_H}{tg\alpha}$$

Area A_1 was defined by key points P_{1I}, P_{10}, P_{2I} and P_{20}, and Area A_2 was defined by key points P_{1H}, P_{2H}, P_{2I} and P_{1I}. Between area A_1 and A_2, an area filled with a radius R_R was created, and the solid model of the rib was constructed.

Bend region modeling. The deformation in the bend region of the loadbeam caused the main difficulties in the parametric modeling. Figure 8 shows the variables for modeling the region. Before the loadbeam was deformed, $L_{00}=12.713$ mm. Given L_{B0}, L_{BC}, L_{T1}, θ, and circular arc length L_{Ar}, we have

$$r_B=\frac{L_{Ar}}{2\pi\theta/360}$$

$$l_{AI}=r_B tg\frac{\theta}{2}$$

$$l_{F0}=L_{BC}+r_B\sin\theta+(L_{00}-L_{BC}-L_{Ar})\cos\theta$$

$$Z_0=(l_{F0}-L_{BC}-l_{AI})tg\theta$$

In the first coordinate system $X_1Y_1Z_1$, we defined the key points

$$P_{BI1}:\{-(L_{00}-L_{BC}-l_{AI}),\quad L_{00},\quad 0\}$$

$$P_{BI0}:\{-(L_{00}-L_{BC}-L_{AI}),\quad 0,\quad 0\}$$

Area A_4 was created by key points P_{BI1}, P_{BI0}, P_{10} and P_{1I}. The second local coordinate system $X_2Y_2Z_2$ was defined with an origin shift ($-l_{F0}$, 0, Z_0). In the $X_2Y_2Z_2$, the defined key points were

$$P_{B01}:\{-L_{B0},\quad L_{00},\quad 0\}$$

$$P_{B02}:\{-L_{B0},\quad 0,\quad 0\}$$

Area A_5 was created by key points P_{B01}, P_{B02}, P_{BI0} and P_{BI1}. An area filled with radius r_B was created between area A_4 and A_5, and the formed section of the loadbeam was modeled. The width and etched region of the bend region were modeled by a similar procedure.

Boundary conditions: The two weld spots between the loadbeam and flexure, and the glued region between the slider and flexure tab were modeled by coupled nodes, i.e., coupled nodes have no relative translational and rotational motions. The dimple was modeled by three coupled DOFs, that is, two nodes (one on the loadbeam, another on the flexure) at the dimple were allowed to have relative rotational motions, and no relative translational motions. The region attached to the base plate of the loadbeam was modeled as nodes restrained to zero displacement.

Entire model and results: The material properties and real constants used in the model are shown in Table 3 . After half of the solid models for the loadbeam, flexure and slider were created, and all lines were meshed by hand, the loadbeam and flexure were automatically meshed by four node shell elements (SHELL63), and the slider was meshed by solid elements (SOLID45). Then, a symmetric reflection about the XZ plane was performed to obtain the entire model. The model is shown in Figure 9. The entire model consists of 1078 shell elements (660 elements for the loadbeam), 12 solid elements, 1284 nodes, and 7553 active DOFs. The modes with frequencies larger than the modal frequencies of the membrane mode are not of interest in our research. Therefore, the modes in the frequency of 0-14000 Hz were calculated using the subspace iteration method. The modal frequencies of main modes are shown in Table 4 (column 5, initial model).

Comparing the results and modifying the model: Comparing the FE model results with the experimental results, we found that: ❶ There were many local modes of the flexure. If the weld spots were expanded in the model, the frequencies of the local modes were increased, but the modes cannot be eliminated. ❷ The modal frequency of the third bending mode was much lower than the experimental value, and there was a large local deformation of the flexure between the two spots in the calculated mode shape of the mode. ❸ The mode shapes were symmetric, which is different with the experimental results.

Based on the experimental and preliminary calculation results, and the practical conditions of the assembly, the model was modified. First, one coupled equation was added to constrain the relative motion in the Z direction between points C_1 and C_2 (shown in Figure 1). Second, the two wire captures at the rail were modeled. There was observed a cut-out of about half the height of the rib nearby the captures. Based on these observations, a modified model was obtained, and used as a basic model in the following analysis. The FE model of the loadbeam is shown in Figure 10. The modal frequencies are shown in Table 4, and the mode shapes are shown in Figures 11 and 12.

Comparing the FE results with the experimental results, we found that:

❶ The calculated modal frequencies of the main modes are very close to the experimental results. The differences for most modes are less than 3%. The largest difference is about 7%.

❷ The calculated mode shapes are very similar to the measured shapes. Especially, the asymmetry in the shapes is consistent. Additional analysis found that the main effects of the captures are the stiffness released by the captures. That indicates the wire captures damage the symmetry of the assembly. The second bending mode was coupled with the first torsional mode (seeing in Figure 12). This will be harmful for the dynamics of the assembly.

❸ The sway mode, shown in Figure 12, was coupled with the torsional mode in the unloaded state. Thus, we can confirm that the measured mode with the frequency of 10327Hz is the sway mode coupled with the torsional mode.

❹ There were still two local modes of the flexure in the analyzed frequency band. One is the local bending mode of the flexure out of phase, another is the local bending mode in phase. This seems reasonable. However, in the experiments we could not find the local modes after many attempts.

In some situations, the loadbeam was modeled in the plane, that is its undeformed state, to simplify the modeling. To simulate this case, $\theta=0.5^0$ was used, and the modal parameters were calculated, which are shown in Table 4. We can see that the frequencies of the sway and torsional modes are much larger than the ones in the case of $\theta=10^0$. Therefore, the flat model cannot suitably simulate the assembly.

3.2 Simulation of the effects of the head load

Effects of the head load. Once the model in the free state has been constructed and verified, it can be used to simulate the effects of head load on the dynamics of the assembly. First, the prestressed large deflection modal analysis was performed to predict their combined effects on the modal parameters. The head load was divided into four components and applied to the four corners of the slider in the Z direction. Under the different loads from 0.5 to 6 grams (increased in increments of 0.5 gram), the θ angle of the rail of the loadbeam and the modal parameters were calculated. Figure 13 shows the

relationship between the angle and the load. We can see that the angle is almost a linear function of the load. The average slope from 2 grams to 4 grams is about -0.157 degree/gram.

Figure 14 shows the effects of the load and deflection on the modal frequencies. When the load was 1.0 gram, the second torsional and third bending modes were coupled with each other. When the load was between 3.5 and 4.0 grams, the second torsional mode was coupled with the local bending mode (out of phase) of the flexure. When the load was between 5.5 and 6.0 grams, the local mode was coupled with the third bending mode. The figure shows that the modal frequencies of the modes coupled with each other are very close in the three ranges of the load. We can see that the second torsional and local bending (out of phase) modes are very sensitive to the load. The frequency of the torsional mode is rapidly increased when the load is increased up to 3 grams. The average slope is about 250 Hz/gram. When the mode was coupled with the local bending mode, the frequency of the second torsional mode rapidly increased, and then gradually decreased with the load. The modal frequency of the sway mode decreased with the load when the load was less than 3.0 grams, with an average slope of -150 Hz/gram. When the load was larger that 4.0 grams, the frequency increased with the load. In addition, we saw that the effects of the load on the mode shapes of the second torsional and sway modes were also significant. The remaining modes were not much affected by the load.

Effects of the prestress. The effects of the load included two parts. One part is the effect of the angle θ change on the modal parameters. Another part is the effect of the prestress

in the assembly on the modal parameters. Therefore, in order to separate the two effects, the modal frequency changes with angle θ alone were calculated. In the free state, the angles in the model were assumed correspondingly equal to the angles under each different load, as shown in Figure 13. The modal frequencies corresponding to the different angles are shown in Figure 15. We can see that the angle significantly affects the modal frequencies of the second torsional and sway modes. The modal frequencies of these modes were increased with the angle.

The modal frequencies in Figure 14 were subtracted from those shown in Figure 15 to determine the effects of the prestress only on the frequencies. The results are shown in Figure 16. The slider's pitch and roll modes were sensitive to the prestress. When the prestress was increased, the frequency decreased by about 3% /gram. The second torsional and sway modes were dramatically affected by the prestress. The main trends were decreasing frequency with the load. The frequency of the sway mode was increased when the load increased beyond 5.0 grams. It is the prestress that results in the discontinuous changes of the modal frequencies in the second torsional and local bending (out of phase) modes when the load changes between 3.5 and 4.0 grams.

3.3 Effects of design variables on modal frequencies

The constructed parametric model can be conveniently used to analyze the sensitivity of the modal parameters to the design variables in the assembly. The relationship between the modal frequencies and the θ angle has been presented in Figure 15. As examples, we investigated the effects of variable L_{Ar}, L_{BC} (bend region, shown in Figure 8); R_H, α (rib

region, shown in Figure 7); and slider location on the modal frequencies. The results are shown in Table 5.

Bend region. The effect of varying L_{BC} and L_{Ar} that define the bend region was investigated. The position of the center of the formed section L_{BC} was shifted from 3.393 mm to 3.647 mm from the center of the base plate. The θ angle and the length (L_{Ac}) of the formed section was fixed ($\theta=10^0$, $L_{Ac}=0.762$ mm). The second torsional mode was the most affected mode. Its frequency decreased by 5.31%. The sway mode was also a sensitive mode, showing a frequency increase of 3.94%. The frequency of the first torsional mode was decreased by 1.74%, and the remaining modes were altered by less than 0.4%.

The length of the formed section was increased from 0.762 mm to 1.016 mm. The angle θ and L_{BC} were fixed. The second torsional and sway modes were also the most sensitive modes to this change, being changed by -2.43% and 2.57%, respectively. The only other notable deviation was found in the first torsional mode (-0.85%). The remaining modes changed by less than 0.3%. Therefore, the sway and torsional modes are significantly affected by the variables of the bend region.

Ribs on the loadbeam. The height (R_H) and the bend angle (α) of the ribs were modified. The height R_H was increased by 0.0254 mm. This modification increased the second and third bending modes by about 4%. The torsional and sway modes were increased by between 1% and 1.7%. The remaining modes were changed by less than 0.5%. The angle

α was increased by 10^o, which resulted in the angle becoming a nearly right angle (88^o). The most affected modes were the sway and torsional modes, the frequencies of which were increased by between 0.39% and 0.67%. The third bending and membrane modes varied -0.32% and 0.38%, respectively.

Location of the slider. The slider was moved forward by 0.1016 mm (about 5% of the length of the slider). The mode most seriously impacted by this change was the slider pitch mode, with a frequency increase of 2.5%. The second and third bending modes were decreased by 0.97% and 0.56%, respectively. When the location of the slider was shifted away from the central line by 0.0762 mm (about 5% of the width of the slider), the frequency of the slider's roll mode was decreased by 0.71%. The change also affected the first torsional mode.

4. Conclusion

1) This report investigated the dynamic properties of the Type 850AK suspension assembly using both experimental and numerical techniques. Good agreement between the FE model and the modal experiments was achieved.
2) In the experiments, six samples with and without wires attached were measured. The statistical results of the modal parameters were obtained, and it was found that the

wires do not significantly affect the modal frequencies and mode shapes, but dramatically increase the damping ratios.

3) A parametric FE model was developed. Using the model, the effects of the head load on the dynamics of the assembly were predicted. The second torsional and sway modes were significantly affected by the load. Therefore, the effects of the large deflection under the head load should be included in the dynamics simulation.

4) By the experiments and FE analysis, it was found that the stiffness reduction resulting from the wire captures at the rail of the loadbeam destroys the symmetry of the assembly, which in turn results in the second bending and first torsional modes becoming coupled to each other. This could be harmful for the dynamics of the assembly.

5) Using the parametric model, the sensitivity of the modal frequencies to the design variables was analyzed. The geometry of the bend region significantly affects the sway and torsional modes. The height of the ribs seriously affects the second and third bending modes, and also affects the sway and torsional modes. Using the parametric model developed here, which was validated by the experiments, design optimization of the assembly will be studied in future research.

ACKNOWLEDGMENTS

This study is supported by the Computer Mechanics Laboratory at the University of California at Berkeley. QHZ also acknowledges the support of the Chinese National Education Committee.

REFERENCES

Harrison J. C., Hanrahan K. P., 1995, “Effect of Mandrel Skew Induced Roll Bias on Suspension Structural Resonance”, Advances in information Storage System, Vol.6, pp29-40, 1995.

Jeans A. H., 1992, “Analysis of the Dynamics of a Type 4 Suspension”, ASME, Journal of Vibration and Acoustics, Vol.114(1), 74-78, 1992.

Diu, D. K., Frees G. M., Gompertz R. S., 1990, "Tracking Dynamics of Read/Write Head Suspensions in High-Performance Small Form Factor Rigid Disk Drives", ASME, Journal of Vibration and Acoustics, Vol.112(1), 33-39, 1990.

Miu D. K., Karam R. M., 1991, “Dynamics and Design of Read/Write Head Suspensions for High-Performance Rigid Disk Drives”, Advances in information Storage System, Vol.1, pp145-153, 1991.

Wilson C. J., Bogy D. B., 1993, “Experimental Modal Analysis of a Miniaturized Suspension/Disk Systems", CML report No. 93-009, Computer Mechanics Lab, Dept. of Mechanical Engineering, Univ. of California at Berkeley, 1993.

Wilson C. J., Bogy D. B., 1994, “Modal Analysis of a Suspension Assembly”, ASME, Journal of Engineering for Industry, Vol.116(3), pp377-386, 1994.

Yong H., Bogy D. B., 1995, “The CML Air Bearing Dynamics Simulator”, CML report No. 95-011, Computer Mechanics Lab, Dept. of Mechanical Engineering, Univ. of California at Berkeley, 1995.

Yoneoka S., Owe T., et al., 1989, "Dynamics of Inline Flying-Head Assemblies", IEEE Tran. on Magnetics, Vol.25(5), pp3716-3718, 1989

Yumura T., Funai K., Yamamoto T, 1991, “A New Design Method of inline Suspensions Based on Dynamic Characteristics”, Advances in information Storage System, Vol.5, pp87-99, 1993.

Zeng Q. H., Bogy D. B., 1996, “Experimental Modal Analysis Technique, System And Application For Miniature Structures”, CML report, Computer Mechanics Lab, Dept. of Mechanical Engineering, Univ. of California at Berkeley, 1996.

No	Mode shape	With wires		No wires		Difference (%)
		Mean (Hz)	Dev. (%)	Mean (Hz)	Dev. (%)	
1	1st Bend	218.82	0.54	218.48	0.71	0.16
2	Roll	1454.3	8.62	1463.5	5.43	-0.63
3	Pitch	1802.2		1815.4		-0.72
4	2nd Bend	2519.9	2.07	2590.7	1.80	-2.73
5	1st Torsion	2745.1	0.16	2798.7	0.83	-1.91
6	2nd Torsion	6695.9	2.96	6854.7	2.13	-2.32
7	3rd Bend	7148.5	1.59	7159.9	0.92	-0.16
8	?	10327	0.99	10385	1.18	-0.56
9	Membrane	12637	0.40	12892	0.34	-1.98
10	4th Bend	14957	1.05	14988	1.11	-0.21

Table 1 Measured modal frequencies of the Type 850AK suspension assembly with wires attached and no wires attached in its unloaded state.

No	Mode shape	With wires		No wires		Difference (%)
		Mean (%)	Dev. (%)	Mean (%)	Dev. (%)	
1	1st Bend	0.2104	22.1	0.0971	10.0	116.6
2	Roll	0.7863	25.6	0.8876	28.1	-11.4
3	Pitch	0.7130		0.7051		1.11
4	2nd Bend	0.7654	39.2	0.1526	19.0	401.7
5	1st Torsion	0.4866	48.6	0.2782	52.7	74.9
6	2nd Torsion	0.5061	28.6	0.1338	20.1	278.2
7	3rd Bend	0.3983	53.5	0.1271	14.1	213.4
8	?	0.4882	19.0	0.2346	45.3	108.1
9	Membrane	0.3909	60.7	0.0789	2.9	395.6
10	4th Bend	0.5401	17.5	0.3706	45.8	45.7

Table 2 Measured modal damping ratios of the Type 850AK suspension assembly With wire attached and no wires attached in its unloaded state.

Component	Loadbeam	Flexure	Slider
Material	Stainless Steel	Stainless Steel	
Young's Modulus(Pa)	1.93×10^{11}	1.93×10^{11}	4.12×10^{12}
Density (kg/m^3)	8030	8030	4250
Poisson's ratio	0.30	0.30	0.27
Real Constants	Thickness .076 mm	Thickness .0305	2.05 x 1.6 x .43 mm

Table 3 Material properties and constants used in the FE model

Mode Shapes	Measured Frequency	FE Model				
		Basic Model		Initial Model	No Wire Captures	Flat model $\theta=0.5$
		Frequency	Diff.(%)			
1st Bend	218.48	211.66	-3.12	211.65	213.27	211.2
Roll	1463.5	1447.4	-1.10	1437.0	1447.6	1453.4
Pitch	1815.4	1787.6	-1.53	1782.6	1788.0	1786.0
2nd Bend	2590.7	2717.9	4.91	2716.5	2767.2	2695.7
1st Torsion	2798.7	2844.8	1.65	2843.9	2868.8	2898.6
2nd Torsion	6854.7	6847.5	-0.11	6752.6	6914.1	8055.0
3rd Bend	7159.9	7070.2	-1.25	6514.2	7130.5	7062.7
Flex. B(O)		8900.0		8045.0	8904.5	9110.0
Flex. B(I)		9364.2		9366.1	9366.9	9366.0
Sway	10385	11119	7.07	11202	11318	12608
Membrane	12892	13020	0.99	13040	13106	12578

Table 4 Modal frequencies of the Type 850AK suspension assembly in its unloaded state

Modal Shape	Modal Frequency	Modal Frequency change (%)					
		Bend Region		Rib Region		Slider Position	
		L_{BC} +.254	L_{Ar} +.254	R_H +.0254	α $+10^0$	X_{SO} +.1016	Y_{SO} +.0762
1st Bend	211.66	0.06	0.00	-0.15	0.14	0.00	-0.01
Roll	1447.4	-0.17	-0.08	0.07	0.01	-0.07	-0.71
Pitch	1787.6	0.03	0.02	0.07	-0.00	2.59	0.13
2nd Bend	2717.9	-0.05	0.04	3.92	-0.10	-0.97	-0.12
1st Torsion	2844.8	-1.74	-0.85	1.71	0.44	0.07	0.31
2nd Torsion	6847.5	-5.31	-2.43	1.50	0.39	-0.10	0.06
3rd Bend	7070.2	-0.37	-0.19	4.34	-0.32	-0.56	0.03
Flex. B(O)	8900.0	-0.30	-0.13	0.09	0.03	0.02	-0.01
Flex. B(I)	9364.2	-0.01	-0.00	0.04	-0.01	-0.14	0.03
Sway	11119	3.94	2.57	1.03	0.67	-0.02	-0.01
Membrane	13020	0.24	0.23	-0.42	0.38	0.01	0.00

Table 5 Modal frequency change for the design variables change of the Type 850AK suspension assembly in its unloaded state

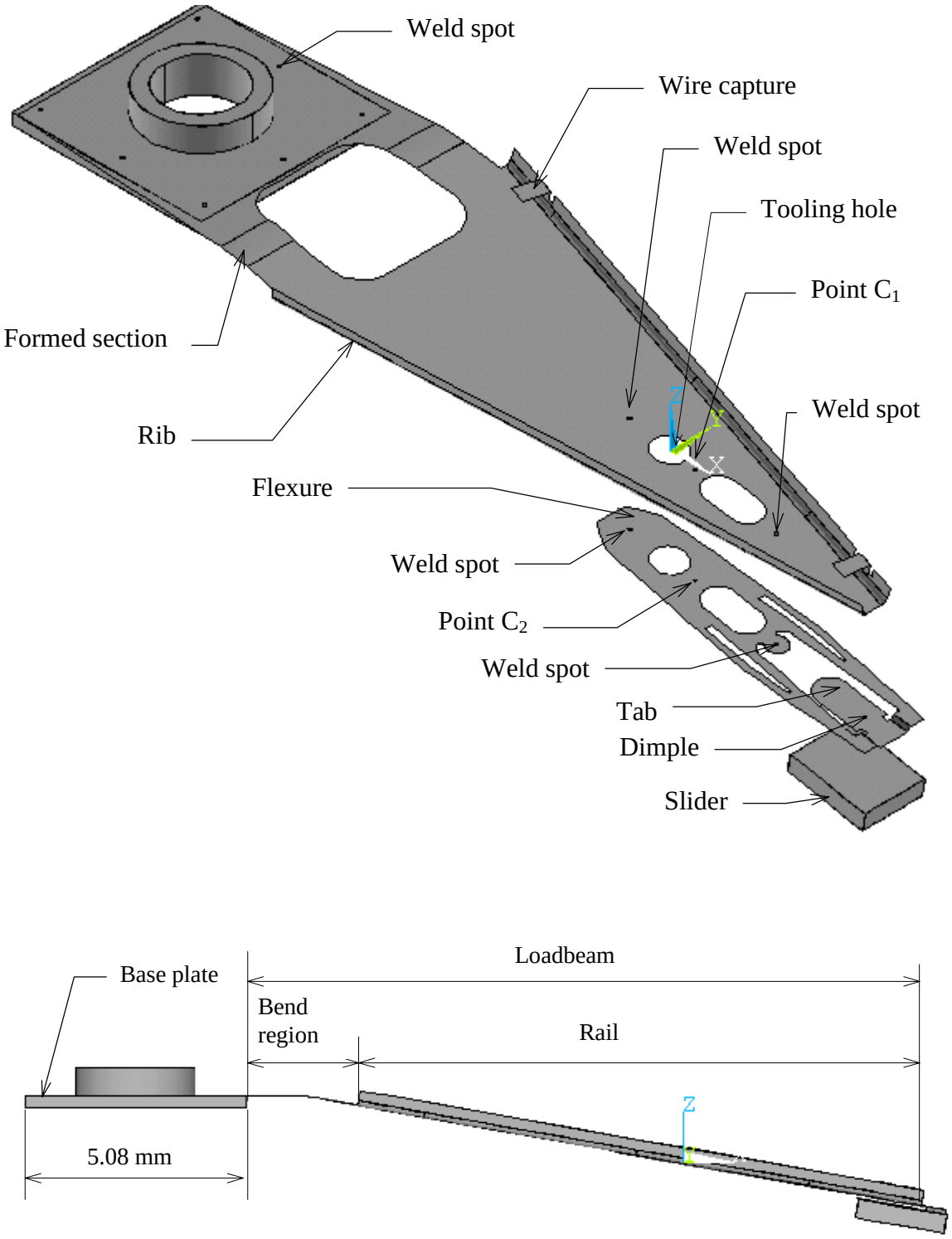

Figure 1 Schematic of the Type 850AK suspension assembly

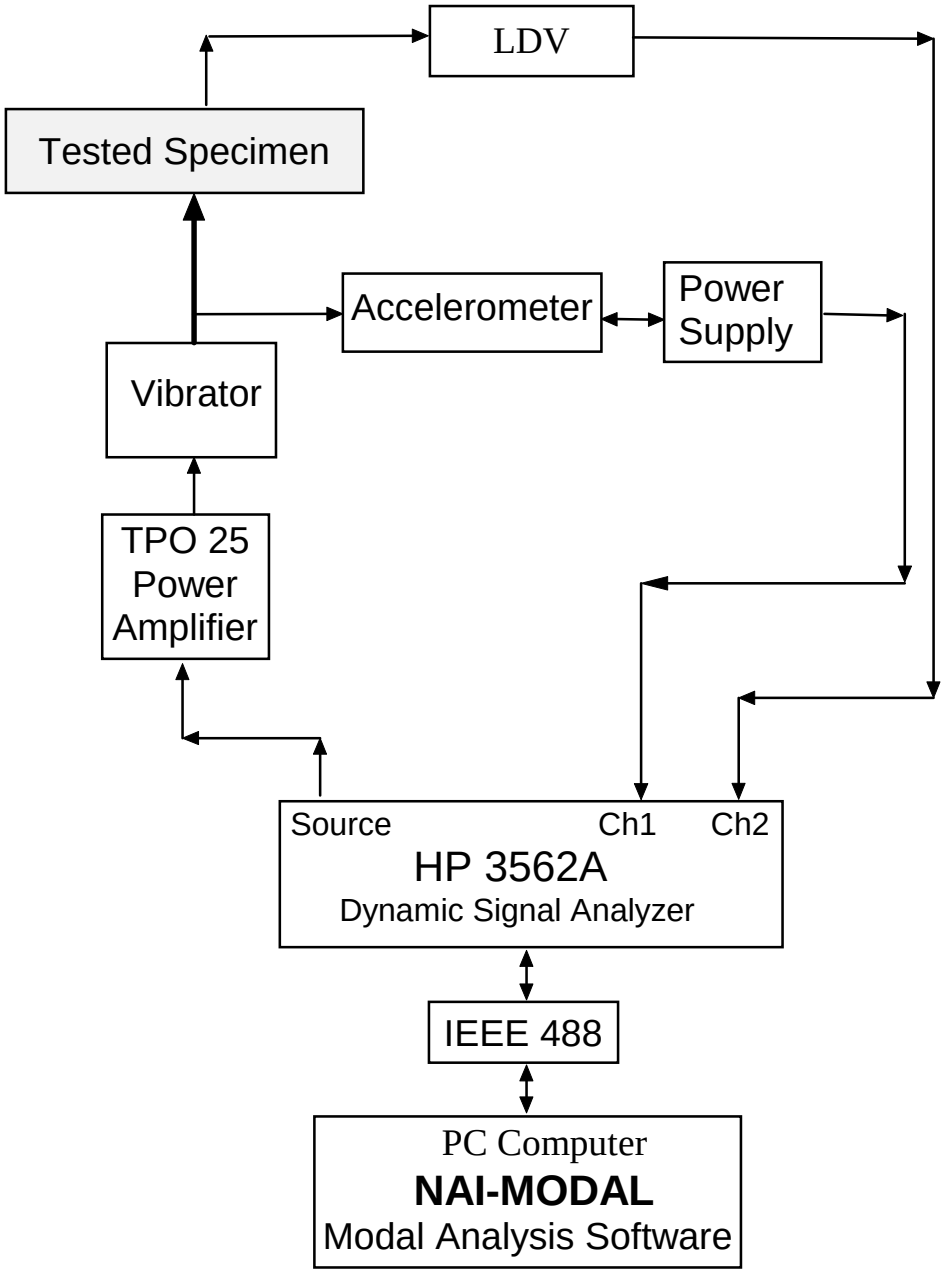

Figure 2 Schematic of the experimental modal analysis system

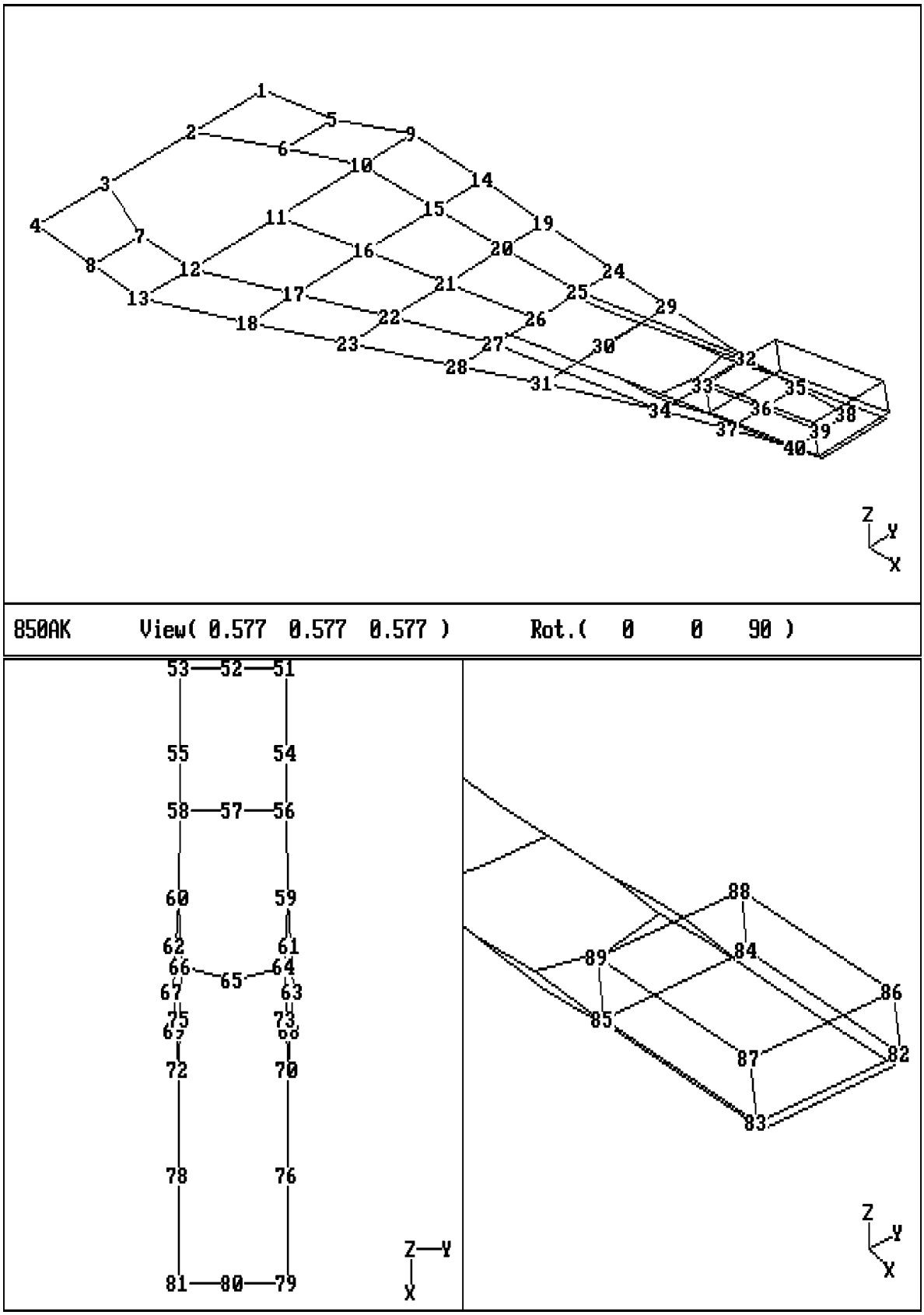

Figure 3 Geometric model of the Type 850AK assembly used in the experiment

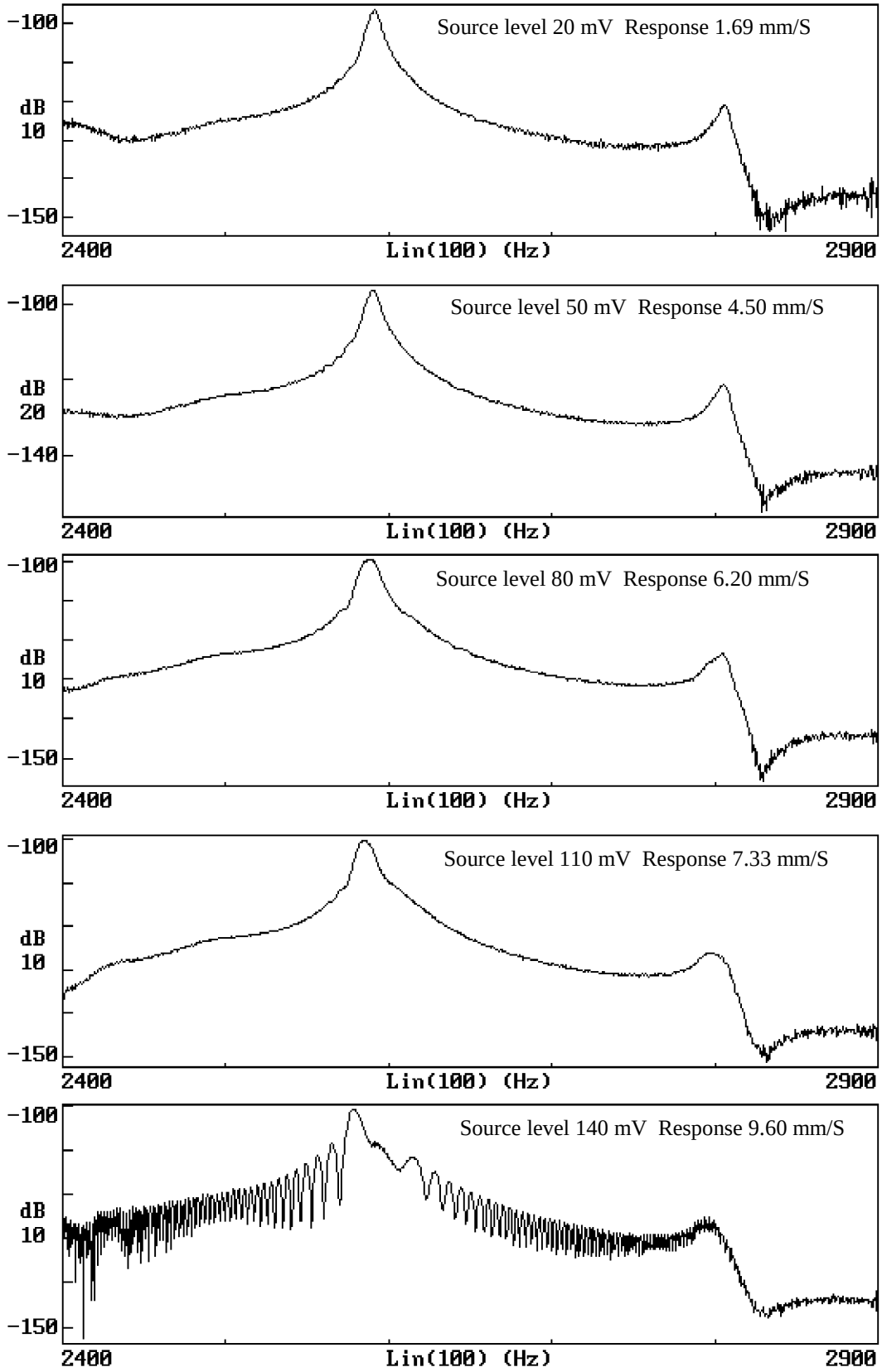

Figure 4 Measured FRFs of the Type 850AK assembly under different excitation levels

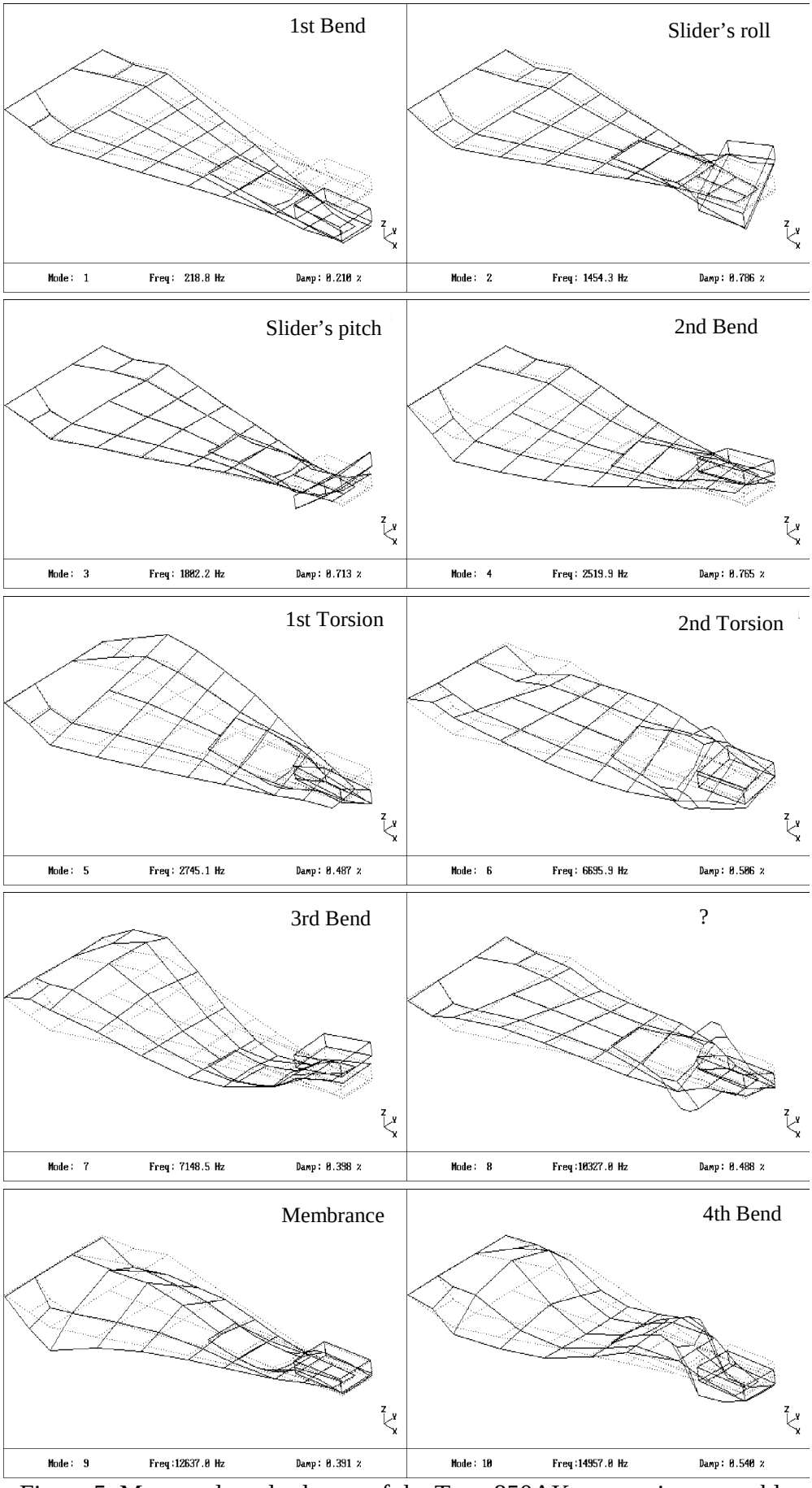

Figure 5 Measured mode shapes of the Type 850AK suspension assembly

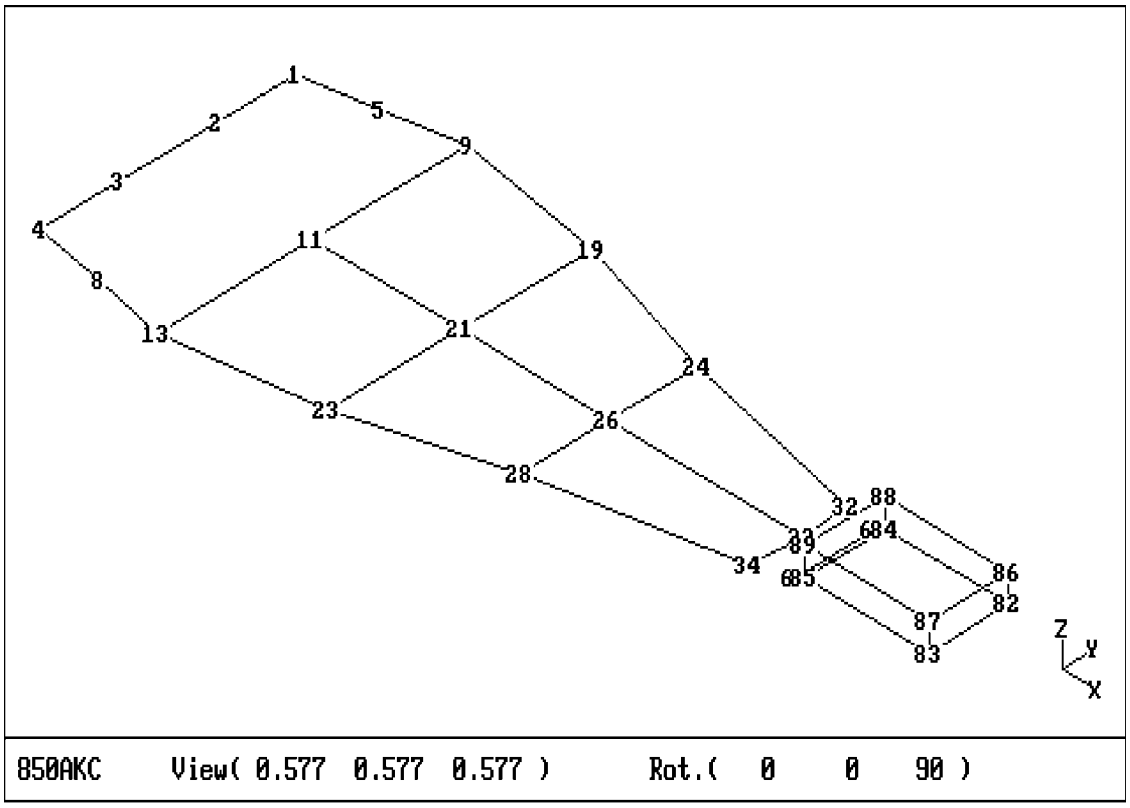

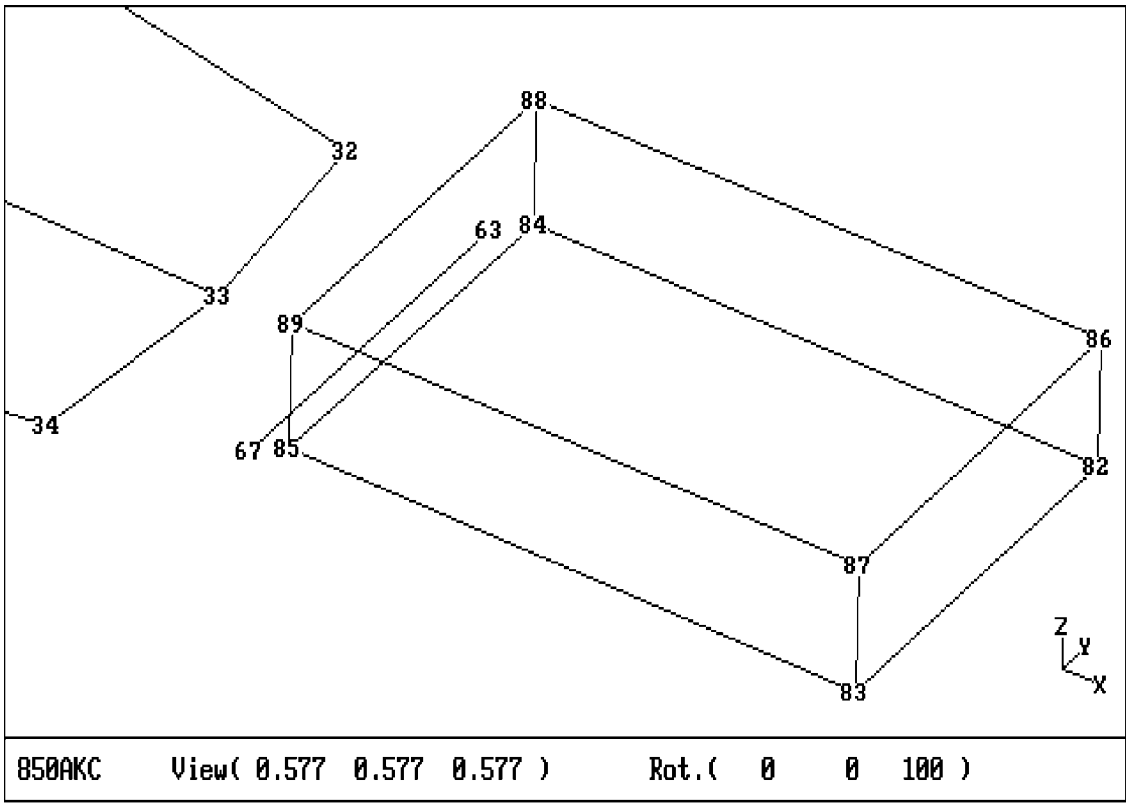

Figure 6 Simplified geometric model used in the experiments

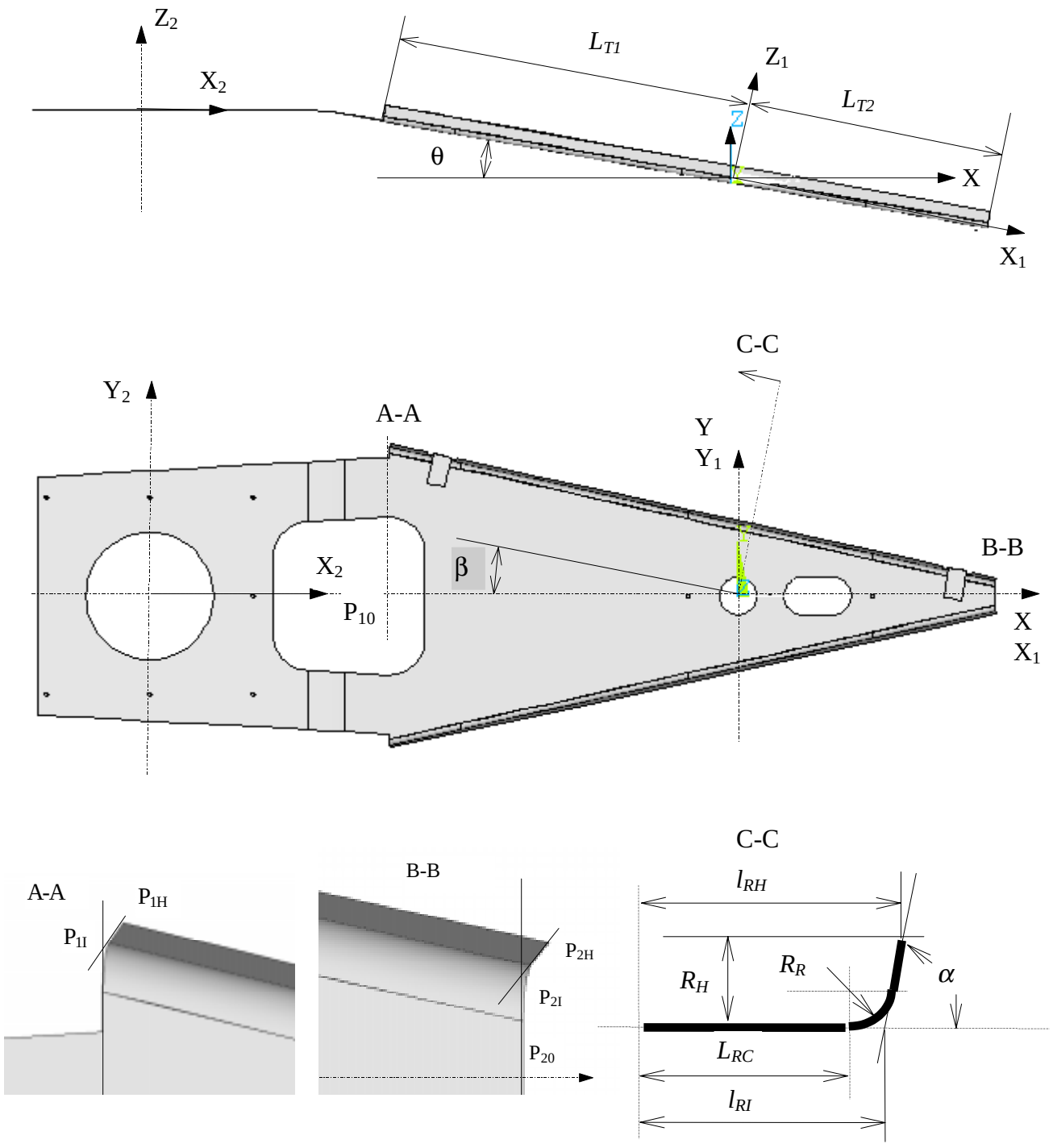

Figure 7 Rib modeling

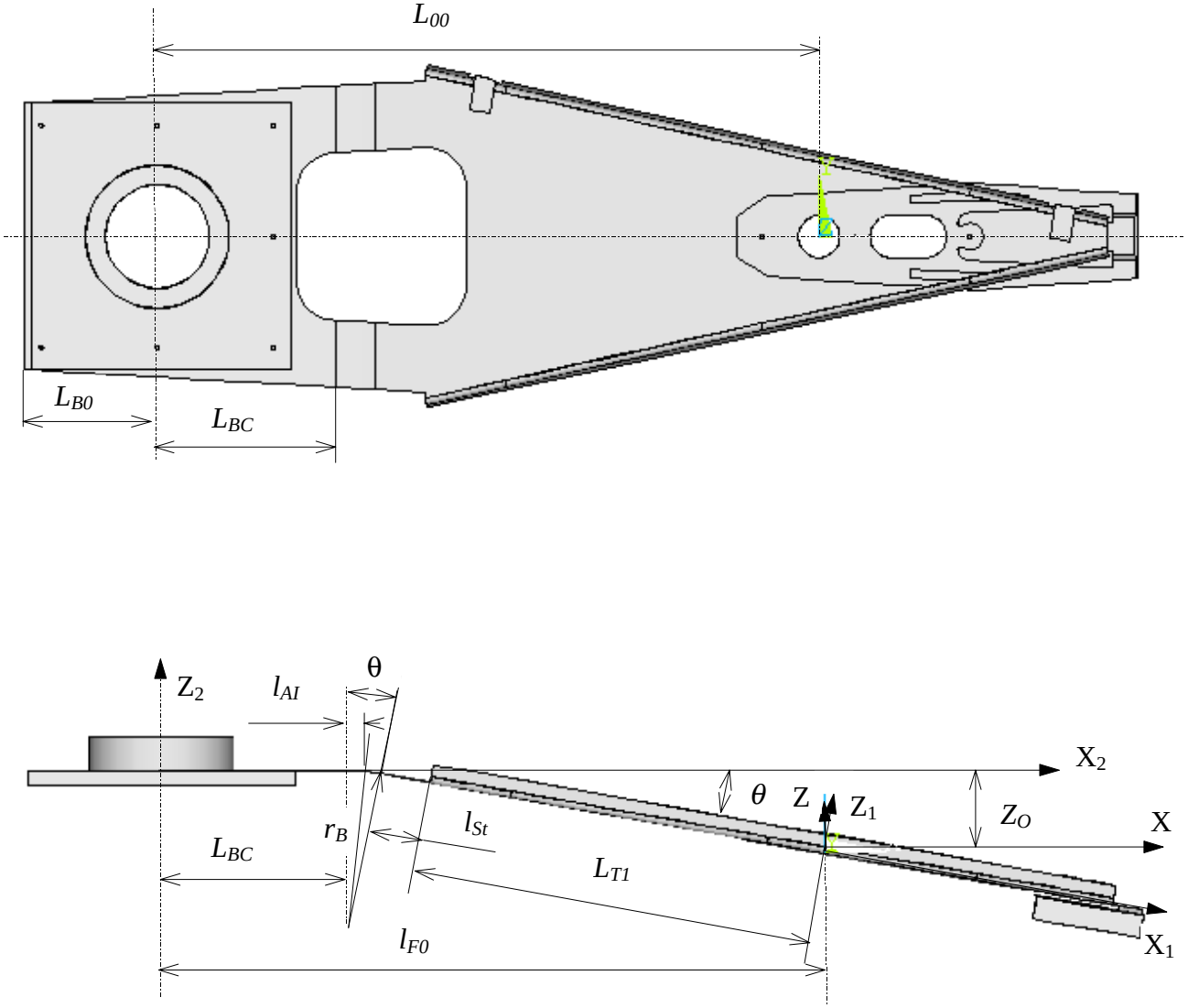

Figure 8 Bend region modeling

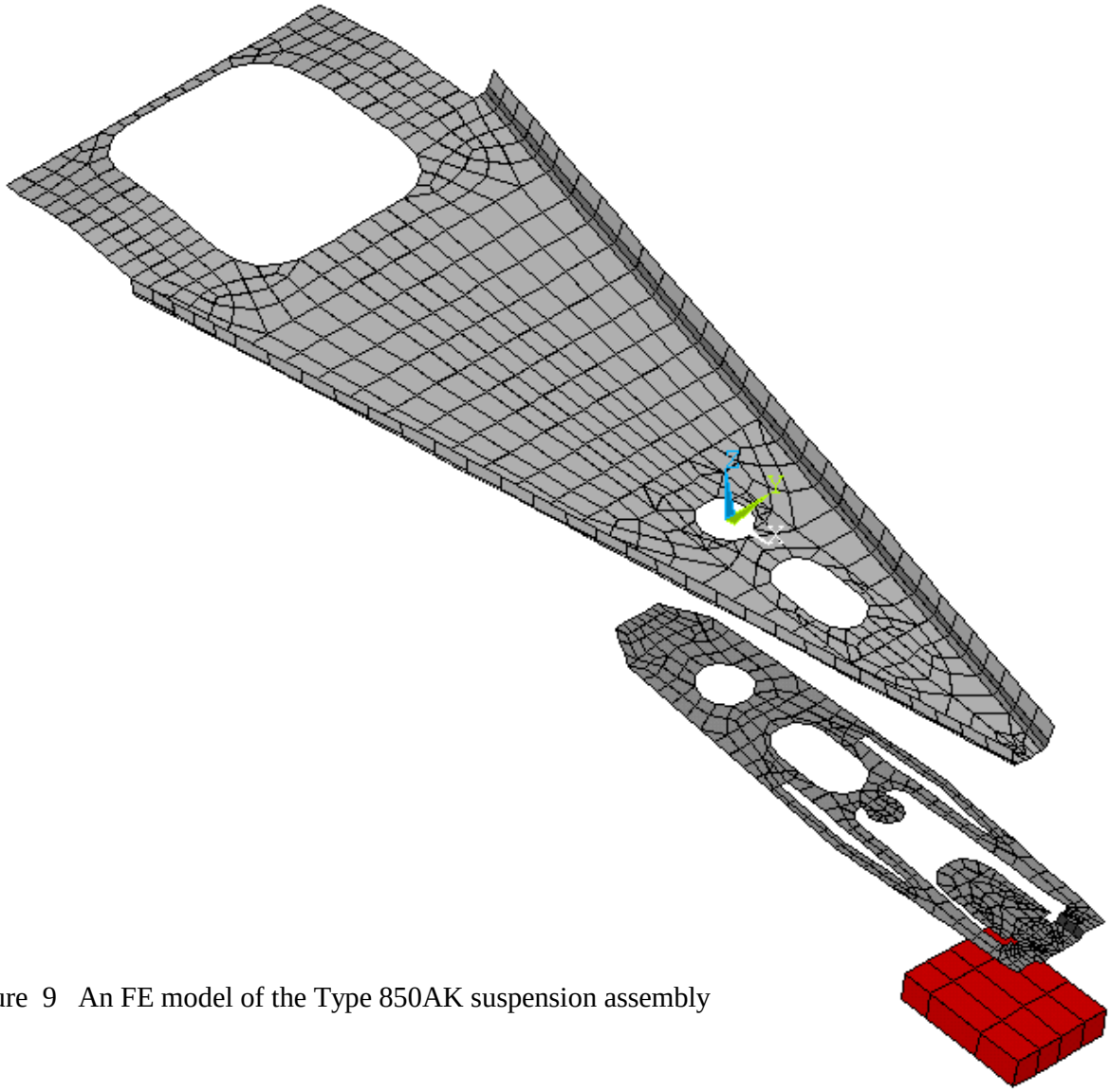

Figure 9 An FE model of the Type 850AK suspension assembly

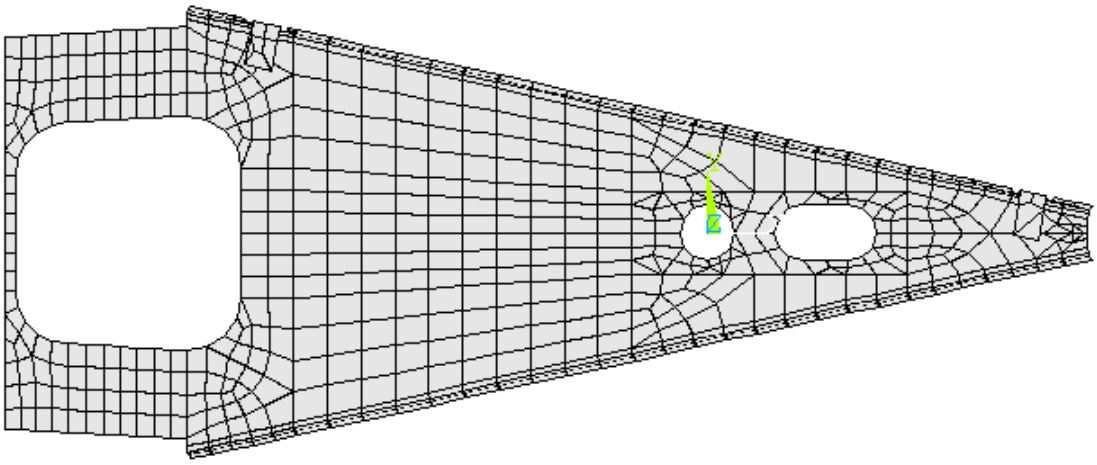

Figure 10 An FE model of the Type 850AK loadbeam (wire captures were modeled)

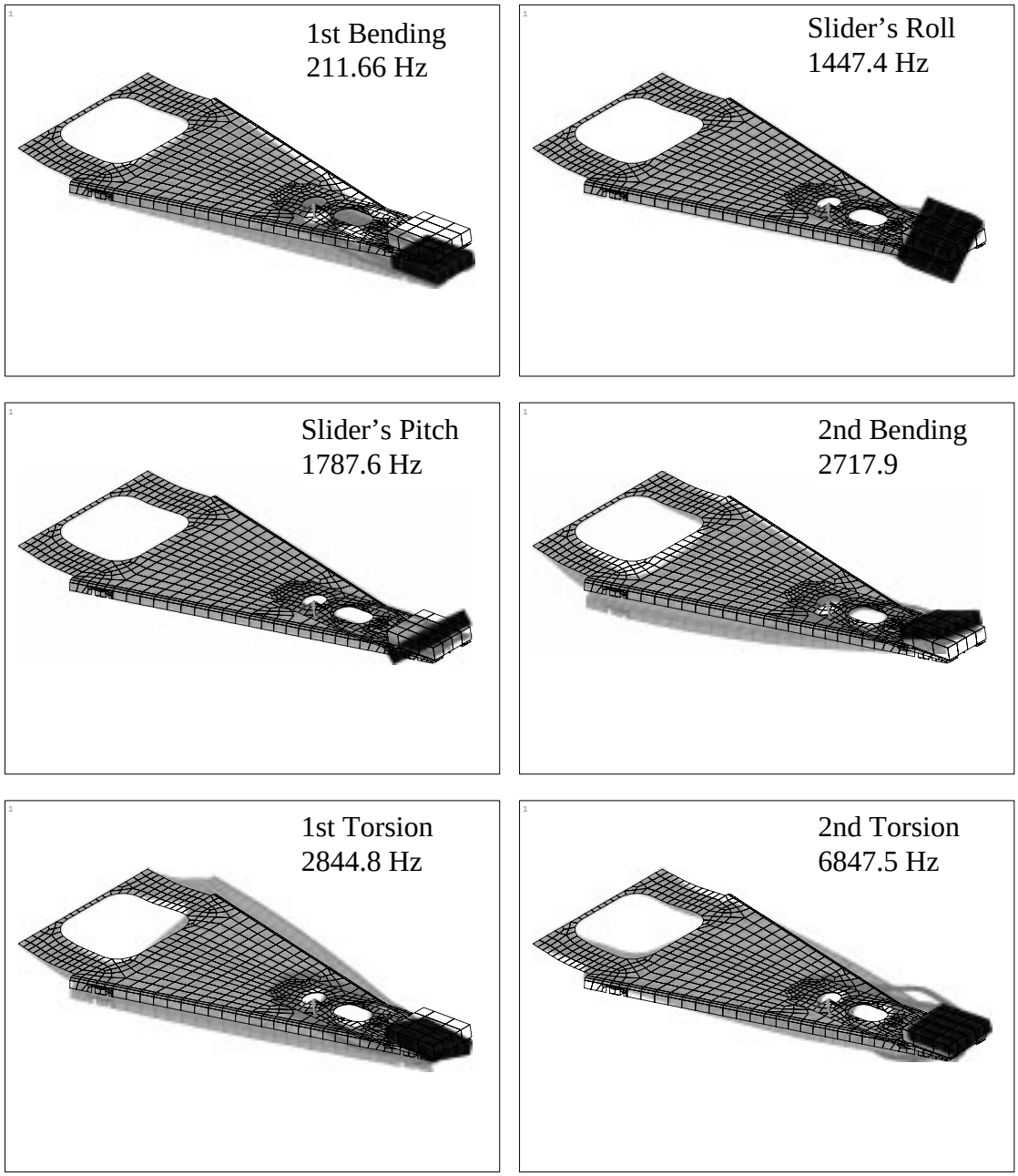

(Continued in next page)

Figure 11 Computational model shapes of the Type 850AK suspension assembly (Deformated & undeformed)

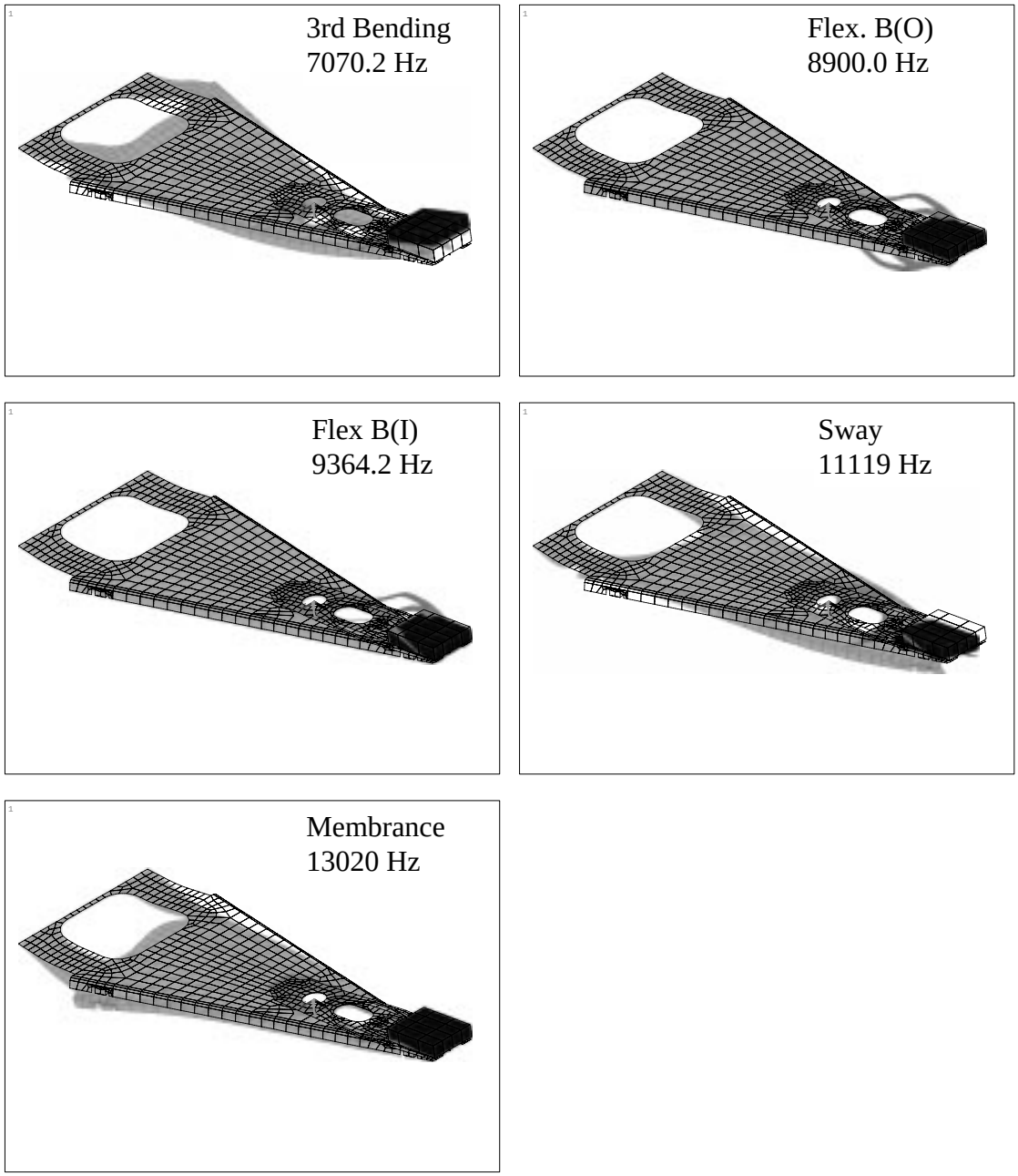

Figure 11(Continued) Computational model shapes of the Type 850AK suspension assembly (Deformated & undeformed)

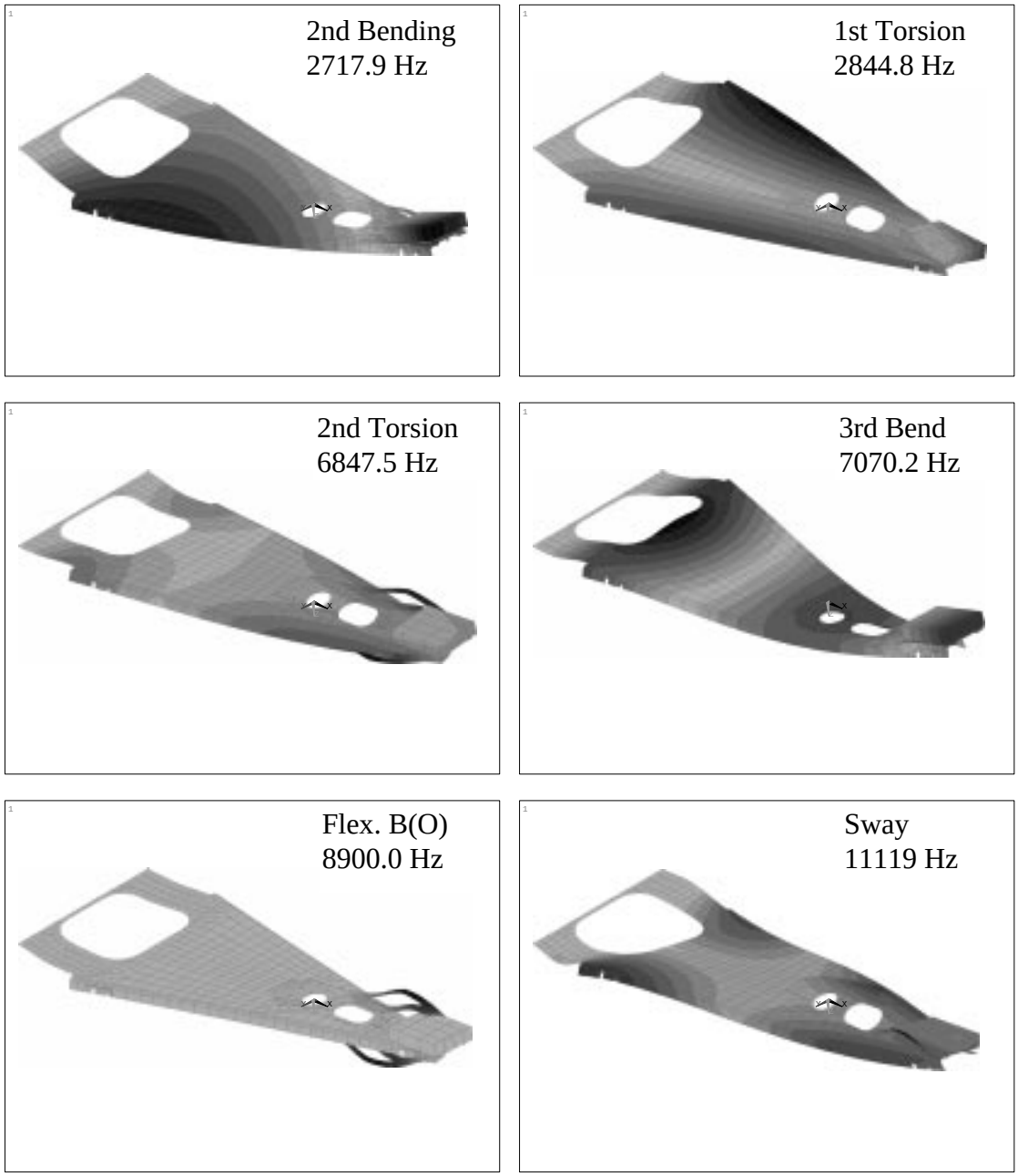

Figure 12 Some computational model shapes of the Type 850AK suspension assembly (Contour display)

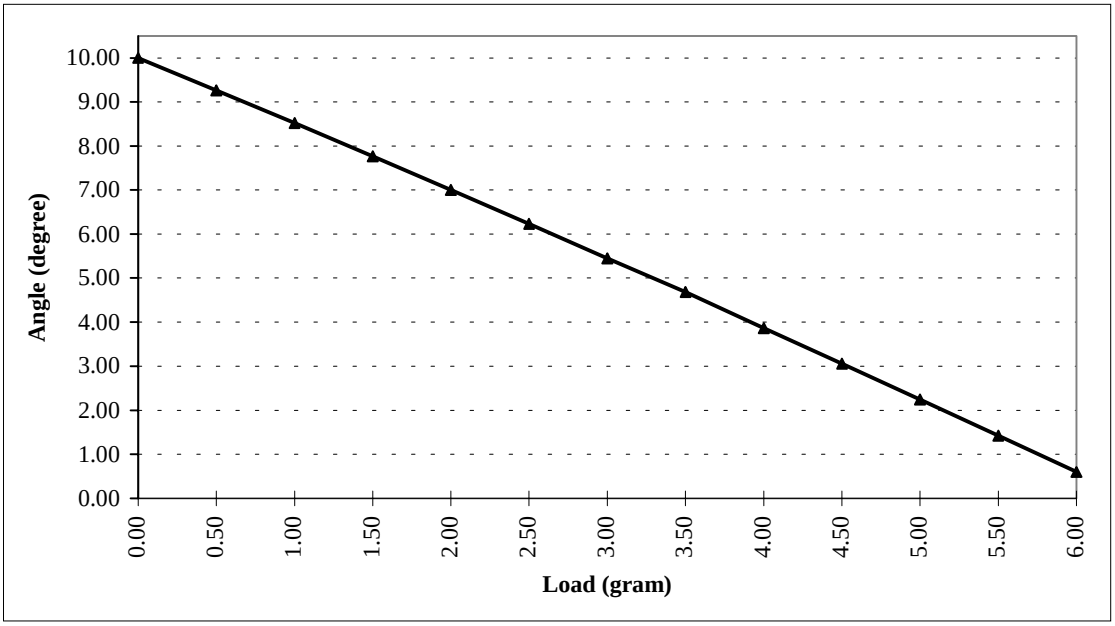

Figure 13 The rail angle θ vs head load

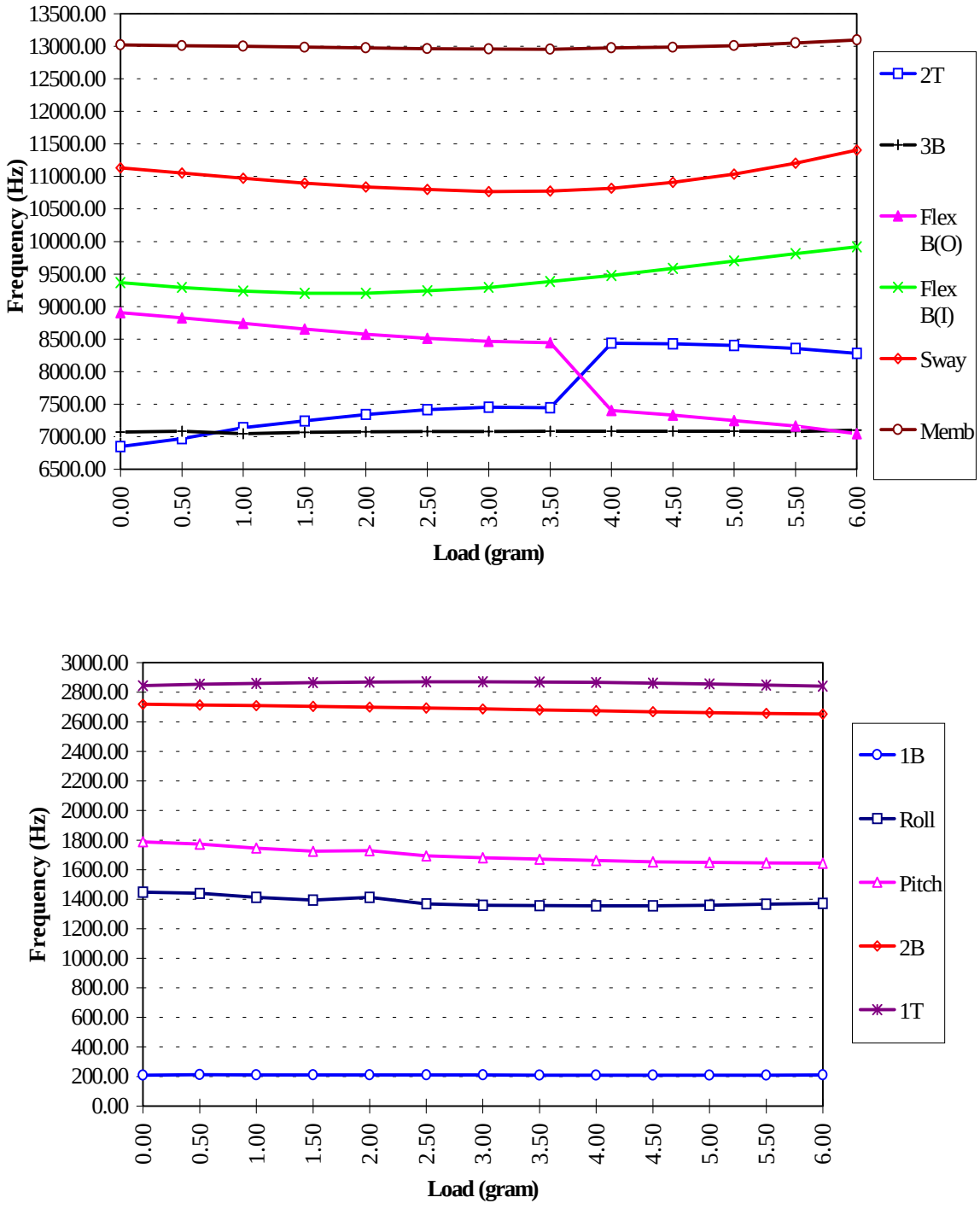

Figure 14 Modal frequency in respect with the head load

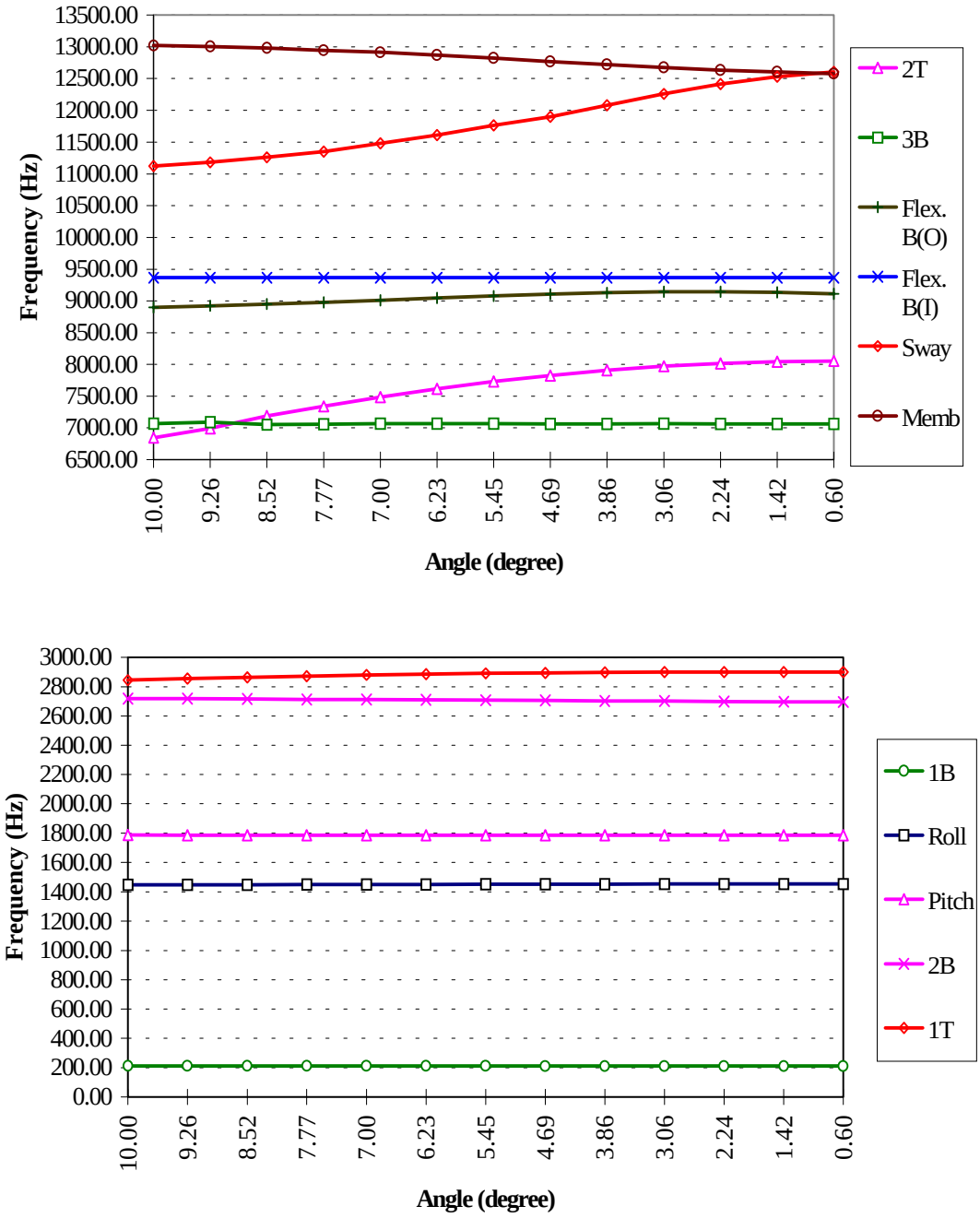

Figure 15 Modal frequency changes corresponding to changes in the rail angle θ

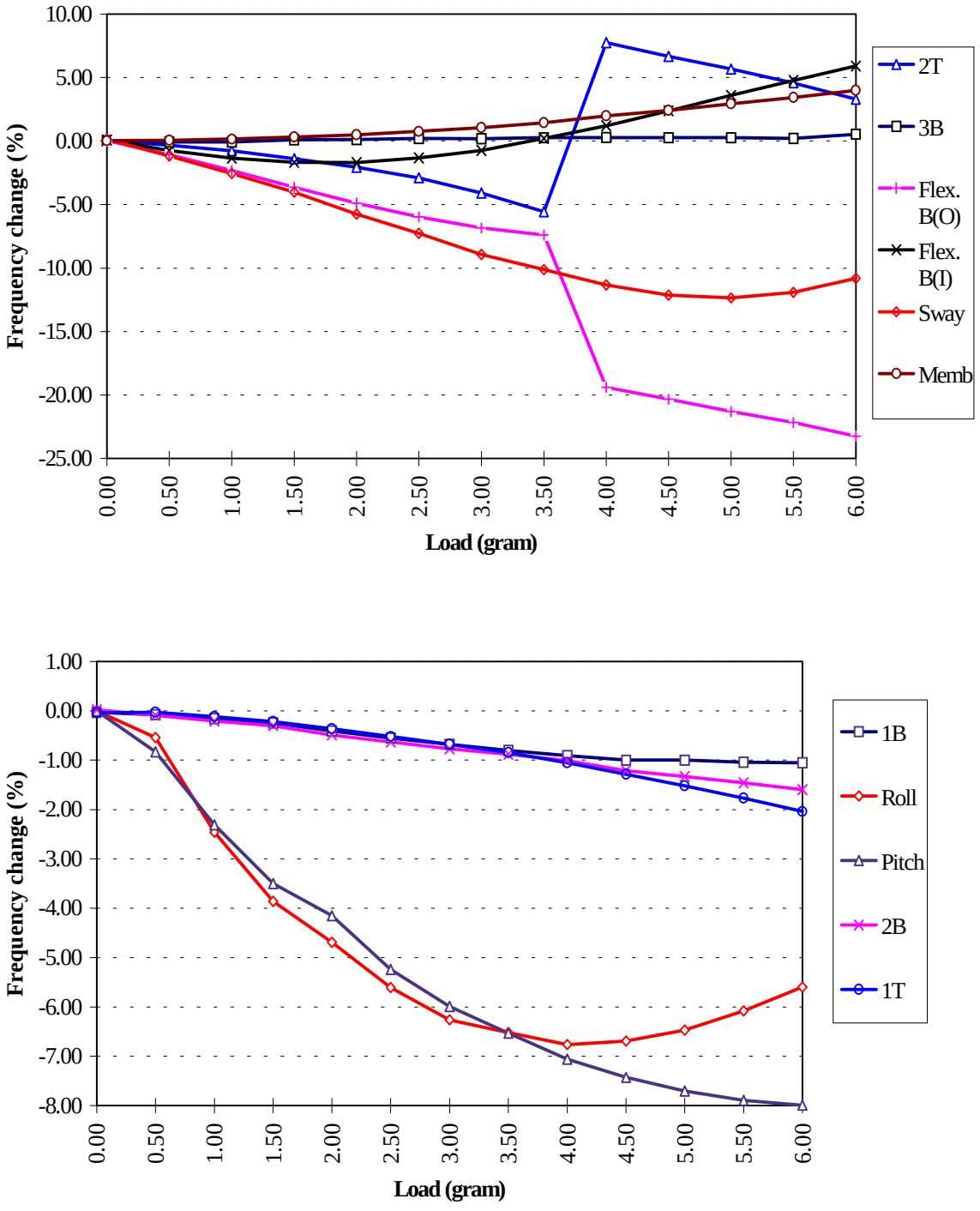

Figure 16 Effects of the prestress on the modal frequency